

# Influence of basis images and skull position on evaluation of cortical bone thickness in cone beam computed tomography



Monikelly do Carmo Chagas Nascimento, DDS, MSc, PhD,<sup>a</sup> Solange Maria de Almeida Boscolo, DDS, MSc, PhD,<sup>a</sup> Francisco Haiter-Neto, DDS, MSc, PhD,<sup>a</sup> Emanuela Carla dos Santos, DDS,<sup>b</sup> Ivo Lambrichts, DDS, MSc, PhD,<sup>c</sup> Ruben Pauwels, DDS, MSc, PhD,<sup>d,e</sup> and Reinhilde Jacobs, DDS, MSc, PhD<sup>d,f</sup>

**Objectives.** The aim of this study was to assess the influence of the number of basis images and the orientation of the skull on the evaluation of cortical alveolar bone in cone beam computed tomography (CBCT).

**Study Design.** Eleven skulls with a total of 59 anterior teeth were selected. CBCT images were acquired by using 4 protocols, by varying the rotation of the tube-detector arm and the orientation of the skull (protocol 1: 360°/0°; protocol 2: 180°/0°; protocol 3: 180°/90°; protocol 4: 180°/180°). Observers evaluated cortical bone as absent, thin, or thick. Direct observation of the skulls was used as the gold standard. Intra- and interobserver agreement, as well as agreement of scoring between the 3 bone thickness classifications, were calculated by using the  $\kappa$  statistic. The Wilcoxon signed-rank test was used to compare the 4 protocols.

**Results.** For lingual cortical bone, protocol 1 showed no statistical difference from the gold standard. Higher reliability was found in protocol 3 for absent ( $\kappa = 0.80$ ) and thin ( $\kappa = 0.47$ ) cortices, whereas for thick cortical bone, protocol 2 was more consistent ( $\kappa = 0.60$ ). In buccal cortical bone, protocol 1 obtained the highest agreement for absent cortices ( $\kappa = 0.61$ ), whereas protocol 4 was better for thin cortical plates ( $\kappa = 0.38$ ) and protocol 2 for thick cortical plates ( $\kappa = 0.40$ ).

**Conclusions.** No consistent effect of the number of basis images or head orientation for visual detection of alveolar bone was detected, except for lingual cortical bone, for which full rotation scanning showed improved visualization. (Oral Surg Oral Med Oral Pathol Oral Radiol 2017;123:707-713)

Cone beam computed tomography (CBCT) has become a commonly used image modality for various applications in dentistry.<sup>1-3</sup> The accuracy of CBCT compared with intraoral radiography has justified its use for cases requiring 3-dimensional (3-D) imaging.<sup>4</sup> It can be of benefit in orthodontics, such as for the evaluation of cortical bone thickness in relation to different facial types, evaluation of detrimental effects on the supporting alveolar bone after orthodontic treatment, and rapid maxillary expansion.<sup>1,4-6</sup>

In periodontics, CBCT images are important to evaluate buccal bone thickness before and after reconstruction of the alveolar buccal bone wall<sup>2,7</sup> and for follow-up of bone augmentation in cases of horizontal bone defects.<sup>8</sup> Moreover, the buccal and lingual cortical bone regions are often evaluated to avoid the risk of

resorption of cortical bone margin in cases of immediate implant placement. This is especially important for maxillary anterior teeth, where cortical bone is thin, and aesthetics is a main factor for the success of immediate implant placement.<sup>9-11</sup>

Recently, studies have demonstrated limitations of CBCT in geometric measurements.<sup>12-14</sup> Thickness and height of cortical bone have been evaluated in prior studies to find the most appropriate method for interpretation and for understanding the limitations of CBCT in the visualization of these structures.<sup>3,15,16</sup> These measurements are often used to evaluate periodontal health or the sequelae of orthodontic treatment. In such cases, a measurement error could lead to a misdiagnosis of bone loss.<sup>14,17,18</sup>

Evaluation of cortical bone is related to several image quality factors.<sup>19,20</sup> Several CBCT units are available on the market, each one manufactured with individual characteristics in relation to acquisition parameters and image visualization. Most CBCT units offer various exposure settings in terms of tube voltage, tube current, exposure time, voxel size, and number of basis

<sup>a</sup>Department of Oral Diagnosis, Piracicaba Dental School, State University of Campinas, Piracicaba, São Paulo, Brazil.

<sup>b</sup>Pontifical Catholic University of Paraná, Curitiba – Paraná, Brazil.

<sup>c</sup>Biomedical Research Institute, Laboratory of Morphology, Hasselt, Belgium.

<sup>d</sup>OMFS IMPATH research group, Department of Imaging & Pathology, University Leuven and Oral & Maxillofacial Surgery, University Hospitals Leuven, Leuven, Belgium.

<sup>e</sup>Department of Radiology, Faculty of Dentistry, Chulalongkorn University, Bangkok, Thailand.

<sup>f</sup>Department of Dental Medicine, Karolinska Institutet, Stockholm, Sweden.

Received for publication Feb 8, 2016; returned for revision Jan 27, 2017; accepted for publication Jan 30, 2017.

© 2017 Elsevier Inc. All rights reserved.

2212-4403/\$ - see front matter

<http://dx.doi.org/10.1016/j.oooo.2017.01.015>

## Statement of Clinical Relevance

This article can contribute to understanding how the different aspects of cone beam computed tomography imaging can influence visualization of anterior cortical bone.

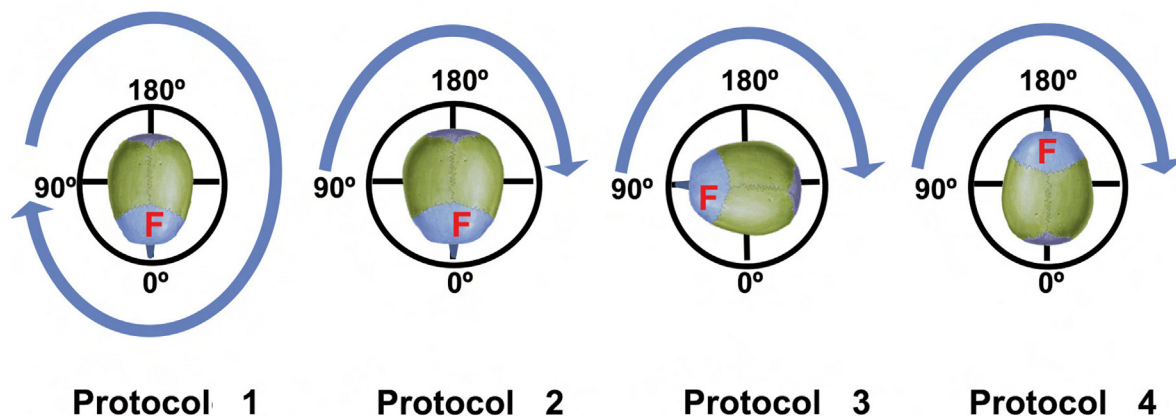


Fig. 1. Different cone beam computed tomography (CBCT) scanning protocols: Protocol 1: 360-degree rotation/Skull position 0°; Protocol 2: 180-degree rotation/Skull position 0°, Protocol 3: 180-degree rotation/Skull position 90°; Protocol 4: 180-degree rotation/Skull position 180°. The letter “F” represents frontal region of the skull (i.e., the location of the cortical bone evaluated in this study).

images.<sup>21</sup> The effect of using a half-rotation scan (i.e., 180-degree rotation of tube-detector arm), which provides an approximately 50% lower number of basis images and a concordant reduction of the radiation dose, on the evaluation of cortical bone is still unknown.<sup>22</sup> Furthermore, the effect of patient orientation versus the X-ray tube and detector for 180-degree rotation protocols has not yet been reported.

The aim of this study was to evaluate the effect of the number of basis images (using full- and half-rotation scanning) as well as the effect of the orientation of the skull for evaluating buccal and lingual cortical bone margins in CBCT.

## MATERIALS AND METHODS

After obtaining ethical approval for the study (protocol No. S55619), preserved dentate dry human skulls were selected. A sample of 11 skulls with 59 intact anterior teeth (23 central incisors, 21 lateral incisors, and 15 canines) was included, fulfilling the following selection criteria: (1) adult skulls, (2) intact skulls with maxillae and mandibles, (3) no metals that could cause artifacts, and (4) no visible pathology. Teeth with different thicknesses of alveolar bone and natural bony dehiscences were selected. A dehiscence was defined as a V-shaped defect along the alveolar bone margin.<sup>16</sup> Cortical thicknesses were measured after taking the tooth out and by using a caliper (Vernier caliper 150, Fujian, China) to classify the cortex as absent (<0.10 mm), thin (0.10-0.50 mm), or thick (>0.50 mm); these measurements served as the gold standard.

Before scanning of the skulls, plastic beads were glued on the lingual and buccal alveolar bone margins to standardize the region to be evaluated. Three cervical vertebrae were added to the skulls.<sup>23</sup> The skulls were then placed in a round plastic basket with a thickness

of 2 mm. A frontal support was used for immobilization of the skull during scanning.

## Image acquisition

Skulls were scanned using the 3D Accuitomo 170 CBCT (J. Morita, Kyoto, Japan). The scanning parameters used were 90 kVp, 87.5 mAs (360° scan, 577 basis images) or 45 mAs (180° scan, 321 basis images), 8 × 8 cm field of view, and a voxel size of 0.16 mm.

Four different scanning protocols were used (Figure 1). A circular paper format divided in 4 quadrants with each row corresponding to a quadrant angle (0, 90, and 180°) was placed on the surface of the scanning platform to guide skull rotation. A copper filter of 1.7 mm thickness was fixed on the X-ray tube to compensate for the lack of soft tissue, as the basket in which the skulls were placed did not provide full simulation of the soft tissue in the head.

## Selection and evaluation of images

Reconstructed CBCT images were exported as DICOM (Digital Imaging and Communications in Medicine) files and then imported into OnDemand 3D software (version 1.0.9 Cybermed, Seoul, Korea) for analysis. The 4 different CBCT protocols were displayed at the same time; the fusion tool was chosen to allow selection of sections at the same position (Figure 2). The images were oriented with the tooth in the vertical position so that the centers of both beads in the labial and buccal cortices were displayed simultaneously on each image. A total of 472 2-dimensional (2-D) sagittal views (59 teeth, 4 scanning protocols, 2 sides) were exported in TIFF (Tag Image File Format). Fifteen images, classified according to their thickness, were then selected from the sample for

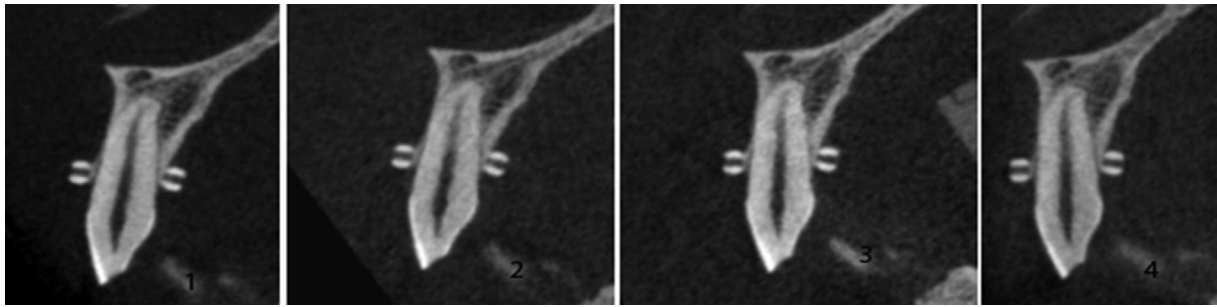


Fig. 2. Tooth scanned using the four protocols according to Figure 1. Full-rotation (360°) with skull rotation of 0° (1), half-rotation (180°) with skull rotation of 0° (2), half-rotation (180°) with skull rotation of 90° (3), half-rotation (180°) with skull rotation 180° (4).

use in observer calibration. Three dentomaxillofacial radiologists were included as observers. Calibration results were analyzed by using the  $\kappa$  test to verify the observers' ability to evaluate the images appropriately. The observers evaluated the images by visual inspection and classified the cortex adjacent to the buccal and lingual beads in each image as absent, thin or thick, using scores of 0, 1, or 2, respectively.

Images were evaluated individually and randomly using ImageJ software (1.45 s version, NIH, Bethesda, MD, USA). To standardize the visualization, the observers were not allowed to change the window level and width, image magnification, and edge enhancement. Observation sessions were performed under dimmed ambient light, with a 22-inch, 2-megapixel clinical review display (MDRC-2122; Barco, Kortrijk, Belgium).

After 15 days, 48 randomly selected images were reexamined by each observer to calculate intraobserver agreement.

### Statistical analysis

Software used for statistical analysis was SPSS 22.0 (IBM, Armonk, NY, USA). Intra- and interobserver agreement were calculated by using the  $\kappa$  test. Observer scores were compared with direct measurements on the skulls, which served as the gold standard. The mode value among the observers was calculated, and the Wilcoxon signed-rank test was used to compare the 4 protocols. The  $\kappa$  test was used to evaluate the scoring in the 3 classifications.

### RESULTS

In all protocols, the highest reliability values were found for the diagnosis of absent cortical bone thickness, and the lowest was observed for the diagnosis of thin cortical bone. The results showed that some thin cortices were diagnosed as having no presence of bone and some thick cortices were diagnosed as thin for all protocols, both for lingual and buccal cortical bone.

The results comparing protocols to the gold standard are shown in Table I. Only protocol 1 (360-degree

rotation) for lingual cortical bone demonstrated no statistically significant difference between evaluations obtained by CBCT images and the gold standard regardless of the condition of cortical bone (absent, thin, or thick).

When evaluating lingual cortical bone, protocol 3 showed the highest agreement among the 4 protocols for absent ( $\kappa = 0.80$ ) and for thin cortices ( $\kappa = 0.47$ ) (Table II). However, for the detection of thick cortical bone, agreement was highest for protocol 2 ( $\kappa = 0.60$ ). The least consistent among the 4 protocols were protocol 2 for absent cortex ( $\kappa = 0.72$ ), and protocol 1 for thin cortex ( $\kappa = 0.37$ ) and thick cortex ( $\kappa = 0.51$ ). With regard to the diagnosis of buccal cortical bone, protocol 1 demonstrated the highest value of correlation among the 4 protocols for absent cortex ( $\kappa = 0.61$ ), while protocol 4 was more concordant for thin cortex ( $\kappa = 0.38$ ) and protocol 2 for thick cortical bone ( $\kappa = 0.40$ ) compared with the other protocols. The least consistent protocols were protocols 2 and 3 for absent cortex ( $\kappa = 0.53$ ), protocol 3 for thin ( $\kappa = 0.32$ ) and protocol 1 for thick cortex ( $\kappa = 0.24$ ).

Intraobserver agreement ranged from very high ( $\kappa = 0.87$ ) to moderate ( $\kappa = 0.50$ ) (Table III) considering different thicknesses. For interobserver agreement, the  $\kappa$  values ranged from substantial ( $\kappa = 0.79$ ) to moderate ( $\kappa = 0.56$ ) (Table IV).<sup>24</sup>

### DISCUSSION

In this study, because of the use of a varying numbers of basis images and orientations of the skull, differences were found when evaluating buccal and lingual anterior cortical bone. Although the 360-degree protocol showed no statistically significant difference in direct measurements for lingual cortical bone, the effect of the number of basis images was inconsistent when considering the different bone thicknesses that were defined for buccal and lingual anterior cortical bone.

Of the previous studies investigating CBCT measurements, several have reported the importance of CBCT on the evaluation of buccal and lingual cortical bone thickness for mini-implant placement, to

**Table I.** Number and frequency (%) for each cortical bone classification of the buccal and lingual cortical bone, in relation to the evaluation obtained from cone beam computed tomography (CBCT) images in each protocol

Cortical evaluation by CBCT	Gold standard (direct measurement)					
	Lingual cortical			Buccal cortical		
	Absent	Thin	Thick	Absent	Thin	Thick
	Protocol 1: Arc 360 degrees/skull 0 degree			Protocol 1: Arc 360 degrees/ skull 0 degree*		
Absent	8 (100)	5 (17)	0 (0)	8 (100)	14 (38)	0 (0)
Thin	0 (0)	16 (57)	7 (30)	0 (0)	21 (58)	13 (86)
Thick	0 (0)	7 (25)	16 (69)	0 (0)	1 (2)	2 (13)
	Protocol 2: Arc 180 degrees/skull 0 degree*			Protocol 2: Arc 180 degrees/skull 0 degree*		
Absent	8 (100)	4 (14)	0 (0)	7 (87)	13 (36)	0 (0)
Thin	0 (0)	21 (75)	8 (34)	1 (12)	22 (61)	12 (80)
Thick	0 (0)	3 (10)	15 (65)	0 (0)	1 (2)	3 (20)
	Protocol 3: Arc 180 degrees/skull 90 degrees*			Protocol 3: Arc 180 degrees/skull 90 degrees*		
Absent	8 (100)	6 (21)	0 (0)	8 (100)	18 (50)	0 (0)
Thin	0 (0)	17 (60)	12 (52)	0 (0)	16 (44)	13 (86)
Thick	0 (0)	5 (17)	11 (47)	0 (0)	2 (5)	2 (13)
	Protocol 4: Arc 180 degrees/skull 180 degrees*			Protocol 4: Arc 180 degrees/skull 180 degrees*		
Absent	8 (100)	5 (17)	0 (0)	8 (100)	17 (47)	0 (0)
Thin	0 (0)	20 (71)	10 (43)	0 (0)	19 (52)	13 (86)
Thick	0 (0)	3 (10)	13 (56)	0 (0)	0 (0)	2 (13)

For direct measurements, cortical bone was defined as absent if <0.10 mm, thin if 0.10-0.50 mm, and thick if >0.50 mm.

\*Significant difference between classification from CBCT observation and direct measurement ( $P < .05$  by Wilcoxon signed-rank test).

**Table II.** Kappa ( $\kappa$ ) values showing agreement between cortical bone classification (absent, thin, and thick) from cone beam computed tomography (CBCT) images and direct measurements used as gold standard

Cortical evaluation by CBCT	Gold standard (direct measurement)					
	Lingual cortical			Buccal cortical		
	Absent	Thin	Thick	Absent	Thin	Thick
	Protocol 1: Arc 360 degrees/skull 0 degree			Protocol 1: Arc 360 degrees/skull 0 degree		
Absent	$\kappa = 0.73$			$\kappa = 0.61$		
Thin		$\kappa = 0.37$			$\kappa = 0.36$	
Thick			$\kappa = 0.51$			$\kappa = 0.24$
	Protocol 2: Arc 180 degrees/skull 0 degree			Protocol 2: Arc 180 degrees/skull 0 degree		
Absent	$\kappa = 0.72$			$\kappa = 0.53$		
Thin		$\kappa = 0.45$			$\kappa = 0.34$	
Thick			$\kappa = 0.60$			$\kappa = 0.40$
	Protocol 3: Arc 180 degrees/skull 90 degrees			Protocol 3: Arc 180 degrees/skull 90 degrees		
Absent	$\kappa = 0.80$			$\kappa = 0.53$		
Thin		$\kappa = 0.47$			$\kappa = 0.32$	
Thick			$\kappa = 0.53$			$\kappa = 0.29$
	Protocol 4: Arc 180 degrees/skull 180 degrees			Protocol 4: Arc 180 degrees/skull 180 degrees		
Absent	$\kappa = 0.74$			$\kappa = 0.58$		
Thin		$\kappa = 0.44$			$\kappa = 0.38$	
Thick			$\kappa = 0.57$			$\kappa = 0.26$

re-establish the buccal bone wall after immediate implant placement, and to detect bone defects.<sup>2,3,13,17,25-28</sup> However, the use of CBCT for these applications should be optimized by balancing diagnostic image quality with radiation dose. The current results show that a 360-degree protocol may not show a distinct advantage over a 180-degree protocol, implying that

the latter would be preferred because of its lower radiation dose (approximately 50% reduction). The main effect of a reduction in the number of basis images is an increase in image noise, but this may not result in an unacceptable diagnostic image, especially in smaller patients. Furthermore, in a clinical setting, a 180-degree rotation would have the additional

**Table III.** Intraobserver agreement results

	<i>Kappa (κ) values</i>
Observer 1	0.64
Absent	0.81
Thin	0.53
Thick	0.60
Observer 2	0.66
Absent	0.80
Thin	0.50
Thick	0.62
Observer 3	0.74
Absent	0.87
Thin	0.70
Thick	0.58

**Table IV.** Interobserver agreement results

	<i>Kappa (κ) values</i>
Protocol 1	0.64
Absent	0.77
Thin	0.56
Thick	0.61
Protocol 2	0.64
Absent	0.71
Thin	0.56
Thick	0.68
Protocol 3	0.70
Absent	0.79
Thin	0.63
Thick	0.66
Protocol 4	0.70
Absent	0.71
Thin	0.56
Thick	0.64

advantage of faster scan times, thereby reducing motion blurring.

Although there is a lot of machine-specific variations, some previous studies have shown that measurements on CBCT were not as accurate as direct measurements of skulls for small structures.<sup>3,5,16,29,30</sup> Loubele et al.<sup>15</sup> even concluded that multislice computed tomography (MSCT) offered better subjective visualization of cortical bone compared with CBCT, although it can be noted that current-generation CBCT models have improved considerably in terms of image quality since then.

The thickness of cortical bone is variable. The anterior maxillary and mandibular regions contain the thinnest cortical bone of the dental arches, generally not exceeding 2 mm, which can hamper its visualization when using CBCT. Thorough analysis of cortical bone, mainly in the aesthetic zone, is recommended to ensure the most appropriate dental implant treatment approach.<sup>31</sup> In some cases, graft insertion may be recommended.<sup>9,32</sup> In this study, the highest κ values were associated with absent cortical bone, which means that it is feasible to diagnose fenestration in cortical

bone with a reasonably high sensitivity. However, the results showed that several thin cortices were diagnosed as having no presence of bone and that several thick cortices were diagnosed as thin, indicating that the amount of bone tends to be underestimated. This underestimation of bone thickness may be caused by the partial volume effect, seeing that gray values in each voxel represent the average attenuation of tissues present in that voxel. Therefore, only voxels that exclusively contain cortical bone appear bright, whereas voxels containing a mix of cortical bone and soft or other tissue will appear darker and may not be perceived as cortical bone by an observer. This causes the outer and inner edges of cortical bone to be blurred, effectively thinning the appearance of cortical bone. It is important to note the markers glued at the surface of cortical bone resulted in a small space between the beads and the cortices, therefore not giving an indication of the distance between the surface of cortical bone and the tooth. A previous study has also reported that measurements, particularly in areas of extremely thin cortical bone, might suffer from some inaccuracy.<sup>3</sup> Additionally, we should consider as an important limitation of this study the fact that scatter radiation produced by soft tissues of a patient or a cadaver in a clinical situation is different from the experimental setup used in this study, mainly when investigating low contrast tissues, such as thin cortical bone.

A previous investigation showed that fenestration in cortical bone was detected on CBCT 3 times more often than on direct skull examination.<sup>16</sup> However, another study found no significant difference between CBCT and direct buccal bone thickness measurements.<sup>33</sup> In the present study, discriminating between bone thicknesses was not of importance, since this would not be relevant from a clinical point of view. Rather, the aim was to show visually if false-positive fenestrations observed on images belonged to fine or thick cortical bone. Accurate information regarding the presence of cortical bone may prevent multiple aesthetic and functional problems in the outcome of implant therapy, independent of the bone thickness present.<sup>17</sup>

Many image quality factors should be considered to explain the limitation of CBCT for this application. The spatial resolution can be considered the minimum distance necessary to distinguish 2 objects located closely together. Commonly, it is incorrectly defined as the voxel size, since some factors, such as partial volume averaging, noise, number of basis images, and artifacts, may influence spatial resolution.<sup>20</sup> CBCT is considered to have a high spatial resolution in comparison to multidetector CT, but its inherently high noise and relatively low contrast resolution may limit proper visualization of small structures. In addition, partial volume averaging is an important factor that often can

occur in cases of thin bone.<sup>34,35</sup> This effect is directly linked to the voxel size. When the voxel size is in the same order of magnitude as the object, visualization is hampered. A smaller voxel size could be more appropriate for these cases.<sup>20,34,36</sup> The voxel size of 0.16 mm used in this study can be considered “high resolution” compared with the voxel sizes used for orthodontic and implant cases, which typically range from 0.2 to 0.4 mm. When thin cortical bone is suspected, it may be necessary to use a smaller voxel size than that used in this study. However, smaller voxels may require a higher radiation exposure (i.e., mAs) to compensate for the concurrent increase in image noise, which would lead to a higher radiation dose to the patient. Further study on the combined effect of mAs and voxel size is warranted to verify whether visualization of cortical bone can be optimized.

Previous studies have shown that a half rotation (180-degree) can reduce the radiation dose to the patient without adversely affecting the diagnosis of periapical lesions, root resorption, and implant planning.<sup>22,37,38</sup> However, images involving both 360-degree and 180-degree rotations of the X-ray source were not able to properly show thin anterior cortical bone in this study, except for images made with 360-degree rotation for visualization of the lingual cortex, which tends to be thicker than buccal cortical bone.

To the best of our knowledge, our study was the first to evaluate the potential effect of skull orientation for 180-degree CBCT scans. Some authors observed that changing the position of the skull did not influence linear landmark measurements when using 360-degree rotation in CBCT.<sup>26,39</sup> In the present study, it was seen that the geometric relationship between cortical bone in the anterior region and the incidence of the X-ray beam does not consistently influence diagnostic image quality. Exposure protocols 2 and 3 (both with an arc of rotation of 180°, involving no skull rotation, and with 90-degree rotation of skull, respectively) showed the best agreement results for lingual cortical bone and buccal cortical bone classified as “thick.” Therefore, from a diagnostic point of view, the current results provide no indication for CBCT manufacturers to change the orientation of the tube relative to the head for 180-degree scans. In terms of radiation dose, it has been shown in a previous study that the effect of anterior versus posterior tube movement for a 180-degree rotation is relatively minor.<sup>40</sup>

## CONCLUSIONS

CBCT showed considerable differences in terms of cortical bone thickness compared with the direct visualization of the skull for all protocols used. A 360-degree arc rotation was, however, able to accurately visualize lingual cortical bone. The orientation of the head versus

the start and end positions of the tube for a 180-degree rotation did not show a consistent effect on image quality.

## REFERENCES

- Ozdemir F, Tozlu M, Germec-Cakan D. Cortical bone thickness of the alveolar process measured with cone-beam computed tomography in patients with different facial types. *Am J Orthod Dentofacial Orthop.* 2013;143:190-196.
- de Molon RS, de Avila ED, de Barros-Filho LA, et al. Reconstruction of the alveolar buccal bone plate in compromised fresh socket after immediate implant placement followed by immediate provisionalization. *J Esthet Restor Dent.* 2015;27:122-135.
- Baumgaertel S. Cortical bone thickness and bone depth of the posterior palatal alveolar process for mini-implant insertion in adults. *Am J Orthod Dentofacial Orthop.* 2011;140:806-811.
- Misch KA, Yi ES, Sarment DP. Accuracy of cone beam computed tomography for periodontal defect measurements. *J Periodontol.* 2006;77:1261-1266.
- Baysal A, Uysal T, Veli I, Ozer T, Karadede I, Hekimoglu S. Evaluation of alveolar bone loss following rapid maxillary expansion using cone-beam computed tomography. *KJO.* 2013;43:83-95.
- Zhao H, Gu XM, Liu HC, Wang ZW, Xun CL. Measurement of cortical bone thickness in adults by cone-beam computed tomography for orthodontic miniscrews placement. *J Huazhong Univ Sci Technol.* 2013;32:303-308.
- Sarnachiaro GO, Chu SJ, Sarnachiaro E, Gotta SL, Tarnow DP. Immediate placement into extraction sockets with labial plate dehiscence defects: a clinical case series. *Clin Implant Dent Relat Res.* 2016;18:821-829.
- Anitua E, Alkhrasat MH, Miguel-Sánchez A, Orive G. Surgical of horizontal bone defect using the lateral maxillary wall: outcomes of a retrospective study. *J Oral Maxillofac Surg.* 2014;72:683-693.
- Katranji A, Misch K, Wang HL. Cortical bone thickness in dentate and edentulous human cadavers. *J Periodontol.* 2007;78:874-878.
- Cook DR, Mealey BL, Veerrett RG, et al. Relationship between clinical periodontal biotype and labial plate thickness: an in vivo study. *In J Periodontics Restorative Dent.* 2011;31:345-354.
- Miyamoto Y, Obama T. Dental cone beam computed tomography analyses of postoperative labial bone thickness in maxillary anterior implants: comparing immediate and delayed implant placement. *Int J Periodontics Restorative Dent.* 2011;31:215-225.
- Hassam B, Souza PC, Jacobs R, Berti SA, Stelt PVD. Influence of scanning and reconstruction parameters on quality of three-dimensional surface models of the dental arches from cone beam computed tomography. *Clin Oral Invest.* 2010;14:303-310.
- Baumgaertel S, Palomo JM, Palomo L, Hans G. Reliability and accuracy of cone-beam computed tomography dental measurements. *Am J Orthod Dentofacial Orthop.* 2009;136:19-28.
- Wood R, Sun Z, Chaudhry J, et al. Factors affecting the accuracy of buccal alveolar bone height measurements from cone-beam computed tomography images. *Am J Orthod Dentofacial Orthop.* 2013;143:353-363.
- Loubele M, Guerrero ME, Jacobs R, Suetens P, van Steenberghe D. A comparison of jaw dimensional and quality assessments of bone characteristics with cone-beam CT, spiral tomography, and multi-slice spiral CT. *Int J Oral Maxillofac Implants.* 2007;22:446-454.
- Leung CC, Palomo L, Griffith R, Hans MG. Accuracy and reliability of cone-beam computed tomography for measuring

- alveolar bone height and detecting bony dehiscences and fenestrations. *AJO-DO*. 2010;137:S109-S119.
17. Arora S, Lamba AK, Faraz F, Tandon S, Ahad A. Rehabilitation of traumatized deficient maxillary alveolar ridge symphyseal block graft placement. *Case Rep Dent*. 2013;2013:748405.
  18. Chan HL, Garaicoa-Pazmino C, Suarez F, et al. Incidence of implant buccal plate fenestration in the esthetic zone: a cone beam computed tomography study. *Int J Oral Maxillofacial Implants*. 2014;29:171-177.
  19. de Moura PM, Hallac R, Kane A, Seaward J. Improving the evaluation of alveolar bone grafts with cone beam computerized tomography. *Cleft Palate Craniofac J*. 2016;53:57-63.
  20. Molen AD. Considerations in the use of cone-beam computed tomography for buccal bone measurements. *Am J Orthod Dentofacial Orthop*. 2010;137:S130-S135.
  21. Ritter L, Mischkowski RA, Neugebauer J, et al. The influence of body mass index, age, implants, and dental restorations on image quality of cone beam computed tomography. *Oral Surg Oral Med Oral Pathol Oral Radiol Endod*. 2009;108:e108-e116.
  22. Lofthag-Hansen S, Thilander-klang A, Grondahl K. Evaluation of subjective image quality in relation to diagnostic task for cone beam computed tomography with different fields of view. *Eur J Radiol*. 2011;80:483-488.
  23. Katsumata A, Hirukawa A, Okumura S, et al. Effects of image on gray-value density in limited-volume cone-beam computed tomography. *Oral Surg Oral Med Oral Pathol Oral Radiol Endod*. 2007;104:829-836.
  24. Landis JR, Koch GG. The measurement of observer agreement for categorical data. *Biometrics*. 1977;33:159-174.
  25. Handelman CS. The anterior alveolus: its importance in limiting orthodontic treatment and its influence on the occurrence of iatrogenic sequelae. *Angle Orthod*. 1996;66:95-109.
  26. Lim JE, Lim WH, Chun YS. Quantitative evaluation of cortical bone thickness and root proximity at maxillary interradicular sites for orthodontic mini-implant placement. *Clin Anat*. 2008;21:486-491.
  27. Berco M, Rigali PH, Miner RM, DeLuca S, Anderson NK, Will LA. Accuracy and reliability of linear cephalometric measurements from cone-beam computed tomography scans of a dry human skull. *Am J Orthod Dentofacial Orthop*. 2009;136:17.e1-17.e9.
  28. Swasty D, Lee J, Huang JC, et al. Cross-sectional human mandibular morphology as assessed in vivo by cone-beam computed tomography in patients with different vertical facial dimensions. *Am J Orthod Dentofacial Orthop*. 2011;139:377-389.
  29. Tsutsumi K, Chikui T, Okamura K, Yoshiura K. Accuracy of linear measurement and the measurement limits of thin objects with cone beam computed tomography: effects of measurement directions and of phantom locations in the fields of view. *Int J Oral Maxillofac Implants*. 2011;26:91-100.
  30. Liang X, Jacobs R, Hassan B, et al. A comparative evaluation of cone beam computed tomography (CBCT) and multi-slice CT (MSCT) part I. On subjective image quality. *Eur J Radiol*. 2010;75:265-269.
  31. Wang HM, Shen JW, Yu MF, Chen XY, Jiang QH, He FM. Analysis of facial bone wall dimensions and sagittal root position in the maxillary esthetic zone: a retrospective study using cone beam computed tomography. *Int J Oral Maxillofac Implants*. 2014;29:1123-1129.
  32. Braut V, Bornstein MM, Belser U, Buser D. Thickness of the anterior maxillary facial bone wall – a retrospective radiographic study using cone beam computed tomography. *Int J Periodontics Restorative Dent*. 2011;31:125-131.
  33. Timock AM, Cook V, McDonald T, et al. Accuracy and reliability of buccal bone height and thickness measurements from cone-beam computed tomography imaging. *AJO-DO*. 2011;140:734-744.
  34. Ballrick J, Palomo M, Ruch E, Amberman BD, Hans MG. Image distortion and spatial resolution of commercially available cone-beam computed tomography machine. *Am J Orthod Dentofacial Orthop*. 2008;134:573-582.
  35. Scarfe WC, Farman AG. What is cone-beam CT and how does it work? *Dent Clin N Am*. 2008;52:707-730.
  36. Fienitz T, Schwarz F, Ritter L, Dreiseidler T, Becker J, Rothamel D. Accuracy of cone beam computed tomography in assessing peri-implant bone defect regeneration: a histologically controlled study in dogs. *Clin Oral Impl*. 2012;23:882-887.
  37. Durack C, Patel S, Davies J, Wilson R, Mannocci F. Diagnostic accuracy of small volume cone beam computed tomography and intraoral periapical radiography for the detection of simulated external inflammatory root resorption. *Int Endod J*. 2011;44:136-147.
  38. Lennon S, Patel S, Foschi F, Wilson R, Davies J, Mannocci F. Diagnostic accuracy of limited-volume cone-beam computed tomography in the detection of periapical bone loss: 360 scans versus 180 scans. *Int Endod J*. 2011;44:1118-1127.
  39. El-Beialy AR, Fayed MS, El-Bialy AM, Mostafa YA. Accuracy and reliability of cone-beam computed tomography measurements: influence of head orientation. *Am J Orthod Dentofacial Orthop*. 2011;140:157-165.
  40. Pauwels R, Zhang G, Theodorakou C, et al; SEDENTEXCT Project Consortium. Effective radiation dose and eye lens in dental cone beam CT: effect of field of view and angle of rotation. *Br J Radiol*. 2014;87:20130654.
- Reprint requests:*  
Monikelly do Carmo Chagas Nascimento, DDS, MSc, PhD  
Av. Limeira  
901, Areião Piracicaba  
São Paulo (SP)  
Brazil 13414-903  
Monikellyccn@gmail.com